Langmuir

Article

pubs.acs.org/Langmuir

Superspreading: Mechanisms and Molecular Design

Panagiotis E. Theodorakis,[†] Erich A. Müller,[†] Richard V. Craster,[‡] and Omar K. Matar*[,†]

[†]Department of Chemical Engineering and [‡]Department of Mathematics, Imperial College London, South Kensington Campus, SW7 2AZ London, United Kingdom

Supporting Information

ABSTRACT: The intriguing ability of certain surfactant molecules to drive the superspreading of liquids to complete wetting on hydrophobic substrates is central to numerous applications that range from coating flow technology to enhanced oil recovery. Despite significant experimental efforts, the precise mechanisms underlying superspreading remain unknown to date. Here, we isolate these mechanisms by analyzing coarse-grained molecular dynamics simulations of surfactant molecules of varying molecular architecture and substrate affinity. We observe that for superspreading to occur, two key conditions must be simultaneously satisfied: the adsorption of surfactants from the liquid−vapor surface onto the three-phase contact line augmented by local bilayer formation. Crucially, this must be coordinated with the rapid replenishment of liquid−vapor and solid−liquid interfaces with surfactants from the interior of the droplet. This article also highlights and explores the differences between superspreading and conventional surfactants, paving the way for the design of molecular architectures tailored specifically for applications that rely on the control of wetting.

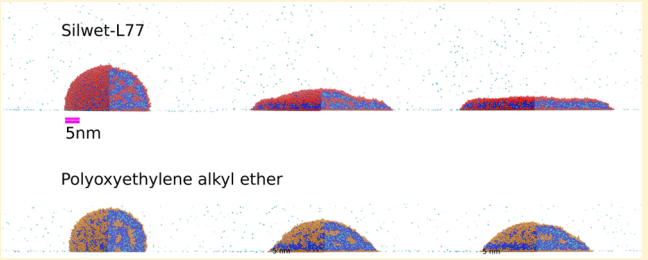

INTRODUCTION

Superspreading is the anomalously rapid and spontaneous wetting of hydrophobic substrates by surfactant-laden aqueous droplets.[1] This phenomenon is of fundamental importance to diverse applications that include, among others, coating technologies, enhanced oil recovery, drug delivery, and herbicides.[2] Despite the earliest reports of superspreading dating back to over 50 years ago,[3] the precise mechanisms underlying this phenomenon remain unclear,[4,5] though a number of factors have been suggested as being relevant.

The first conundrum is why only some siloxane-based surfactants exhibit this behavior.[6] In that sense, the peculiar T-shaped geometry of the known superspreading trisiloxane surfactants is often cited[1,7] as the enabling factor in the formation of a bilayer near the three-phase contact line (CL). This surfactant bilayer is thought to "sandwich" water molecules and accelerate their spreading over the surface.[8] The abnormally rapid adsorption of surfactant molecules directly into the CL aided by Marangoni effects has also been postulated as a prerequisite for superspreading by a recent continuum-scale study.[9,10]

Experiments have explored individually the plethora of factors that may aid or suppress superspreading, such as rate of evaporation,[11] humidity,[1,12] pH,[13] surfactant structure and concentration,[14,15] surfactant aging effects,[16] surfactant mixtures,[17,18] substrate hydrophobicity,[1,12,19] and temperature,[12,20] but in general have failed to give a complete molecular picture of the underlying mechanisms for this unique behavior. One could envisage that this understanding could come about from molecular dynamics (MD) simulations at the atomistic level. Current and foreseeable computational power, however, is insufficient to cover the size and length scales required to model the spreading of even the smallest nanoscale drops. For example, an MD simulation based on an all-atom force field found that trisiloxane surfactant-laden droplets spread very little on graphitic substrates despite being able to form bilayers in an aqueous solution. In contrast, alkyl polyethoxylate surfactant-laden droplets were found to spread significantly further,[21] which is in contradiction to what is expected from experiments.[1] This result was partially attributed to the limitations in time and length scales accessible to simulations.[21] To address this, one needs to resort to coarse-graining the irrelevant degrees of freedom but then employ a force field that describes fluid−fluid and fluid−solid interactions quantitatively in order to have the required level of correspondence with experiments. The approach has shown promising results[22,23] and trends that are in line with experiments. For example, it has been found that the T-shaped geometry of the surfactant leads to the formation of bilayers and considerably favors the spreading of droplets. However, no details with respect to superspreading mechanisms are given in those studies.

To isolate the mechanism, we develop large-scale coarse-grained MD simulations of droplets of aqueous solutions of Silwet-L77, (a well-known superspreader) using the SAFT[24] force field. (See the Supporting Information for a detailed description and validation of the SAFT models.) The level of coarse-graining, the large simulation sizes, and the extended time allow us to obtain, for the first time, a picture of the

Received: November 18, 2014
Revised: January 27, 2015
Published: February 6, 2015

DOI: 10.1021/la5044798
Langmuir 2015, 31, 2304−2309

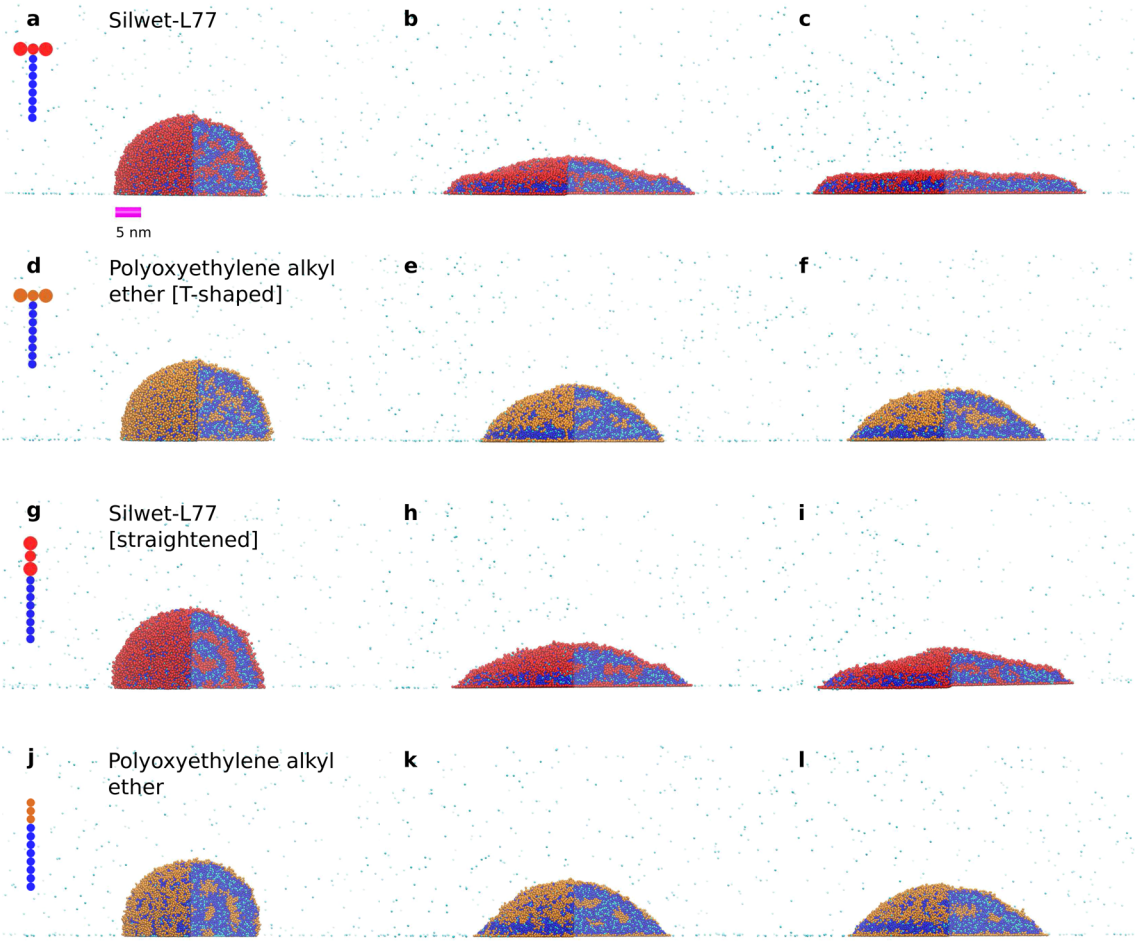

Figure 1. Superspreading. Different stages of the superspreading process at 0τ, $7 \times 10^4\tau$, and $14 \times 10^4\tau$ (time increases from the left to right column) for Silwet-L77 (a–c), an exemplar conventional polyalkylether surfactant with T-shaped geometry (d–f), a straightened Silwet-L77 (g–i), and an exemplar conventional linear surfactant polyalkyether surfactant (j–l). Red (M or D effective beads, with D being the central bead) or orange (CM effective beads) denotes the hydrophobic effective beads, blue denotes the hydrophilic EO effective beads, and cyan denotes the water molecules (Supporting Information). Droplets have the same surfactant concentration, namely, 8.3CAC, which is above the critical wetting concentration (CWC). One-quarter of the droplet has been removed from the snapshots in order to show the external structure of the LV interface and the interior of the droplet for each case.

superspreading mechanism. Moreover, understanding the pivotal differences between superspreading (Silwet-L77) and nonsuperspreading molecules (e.g., polyalkylether surfactants) allows us to determine the molecular design of the mentioned surfactants.

METHODOLOGY

We employ MD simulations of a coarse-grained model in the canonical ensemble as implemented in the HOOMD-blue package.[25] A temperature of $T = 25$ °C is fixed throughout by a Nosé-Hoover thermostat. Simulation lengths depend on the spreading rate and extent of the spreading but typically last for over $(5-10) \times 10^4$ τ, where τ is the time unit. The simulation box is rectangular in shape, bounded by a bottom surface (substrate) of dimensions $L = 131$ nm in each of the directions of the plane with periodic boundary conditions applied in these directions. Perpendicular to the plane, the size of the simulation box is 78 nm and its upper bound is a repulsive wall; no periodic boundary conditions are applied in the z direction.

The coarse-graining methodology smears out the atomistic details and substitutes them with a model based on a collection of spherical beads which, in the case of the surfactants, are linked in linear and branched geometries. Each bead roughly corresponds to a similar molecular weight and encompasses between three to five heavy atom centers. In excess of 80 000 individual beads are included in any given simulation, corresponding to $O(10^6)$ atoms. In our study, a bead denoted as "W" represents two water molecules[26] (H_2O), effective beads "M" represent a chemical group $(CH_3)_3{-}Si{-}O_{1/2}$, and an effective bead "D" corresponds to the group $O_{1/2}{-}(CH_3)_2{-}Si{-}O_{1/2}$. "EO" effective beads represent $-CH_2{-}O{-}CH_2-$ (ether) chemical groups, while "CM" effective beads correspond to $-CH_2{-}CH_2{-}CH_2-$ (alkane) chemical groups.[27] No distinction is made between terminal methyl groups and CH_2 groups. The nonbonded interactions are regressed from pure component thermophysical data (typically densities and vapor pressures) of smaller chemical moieties using an analytical equation of state (EOS) and the statistical associating fluid theory (SAFT).[24,28] One of the key issues in developing coarse-grained force fields is the methodology used to parametrize the intermolecular potential, i.e., what values of ε, σ, and so forth to use and where to regress them from. At one end of the spectrum, one can think of coarse-graining as a way of upscaling an atomistic simulation or a finer-resolution model, reducing

DOI: 10.1021/la5044798
Langmuir 2015, 31, 2304–2309

the number of degrees of freedom and effectively integrating the detail. A review of some of these so-called "bottom-up" approaches[29] unequivocally discusses how these approaches have issues in terms of the transferability and "representability" of the potential parameters to scenarios that have not been fitted. A fundamentally different "top−bottom" approach is used herein, as the potential parameters are optimized to reproduce the macroscopically observed thermophysical properties, namely, the saturated liquid density and the vapor pressure of selected compounds. This is done by employing an equation of state (an analytical representation of the free energy corresponding to the given interaction potential). Very few coarse-grained force fields provide both the level of flexibility (large parametrization set) and accuracy to be used in quantitative simulations such as the ones described here. The MARTINI[30] force field is a possible example. This force field has been adjusted to fit the oil−water partition coefficients and is a prime example of excellent parametrization. In this particular application, however, it presents several deficiencies, namely, in the description of the tension of pure water, the failure to account for beads of different sizes, and the lack of parameters for all moieties required. The SAFT force field does not suffer from the aforementioned limitations and has been shown to reproduce in a quantitative manner the behavior of complex fluids and, of particular interest to this case, ethoxylated surfactants and photosensitive surfactants in water.[31]

In our study, the surfaces correspond to unstructured walls with an integrated potential that depends only on the energy potential parameters and the distance to the surface.[32] The baseline surface is paraffinic in nature, parametrized so that a pure water droplet has an average contact angle of 60°, corresponding to the conditions for which the optimum superspreading behavior is observed experimentally.[1] Details of the force fields, parameter values, and validations are given in the Supporting Information.

Results are expressed in reduced units to be able to scale to macroscopic observables. The average surfactant concentration is expressed in multiples of the critical aggregation concentration (CAC, see Supporting Information). Our simulations start with a preliminary simulation of the droplet with surfactant, where the formation of the droplet and the deposition of it onto the substrate take place. During this initial simulation, we choose a weak attraction of the surfactant to the substrate in order to avoid droplet spreading. After this initial stage, the interactions of the surfactants with the substrate are switched on and the droplet starts spreading with a rate that depends on the surfactant's affinity on the substrate for a given wettability. During spreading, we gather samples of droplet configurations at the same regular intervals. By using a cluster analysis algorithm, we find, for each configuration, the effective beads that belong to the droplet and calculate all of the reported properties. Further details are presented in the Supporting Information.

RESULTS AND DISCUSSION

The simulations for Silwet-L77 confirm the hypothesis[8] suggesting the existence of a bilayer (Figure 1b) that forms in the initial stage of superspreading at the CL. We observe that this bilayer grows continuously and persists until the completion of the spreading process (Figure 1c). In this final stage, the droplet has spread to form a thin film, where all of the surfactant molecules have adsorbed either at the liquid−vapor (LV) or solid−liquid (SL) interfaces surrounding the water molecules (Figure 1c).

In the SAFT coarse-grained representation, Silwet-L77 consists of three head beads, representing the essentially hydrophobic siloxane groups and a perpendicular (hence the name "T-shape") tail of eight beads representing the hydrophilic ethoxylated moieties. Surfactant-laden aqueous drops are placed on flat, unstructured surfaces of varying fluid−solid energies to analyze, among other properties, the time-dependent spreading and final equilibrium configurations. The "baseline" simulation corresponds to Silwet-L77 on a paraffin-like hydrophobic substrate. The latter is a typical superspreading scenario[12] (Figure 1a-c, Supporting Information video), with a final state of complete wetting.

To assess the influence of the molecular architecture of Silwet-L77 on spreading, we reconnect the hydrophobic beads of this molecule in such a way as to obtain a surfactant of linear architecture (Figure 1g), that is, a "straightened" Silwet-L77, without changing the interactions between effective beads. Notwithstanding the existence of a bilayer (Figure 1i), the spreading is completed at a later time (not shown in the figure). Moreover, this linear surfactant cannot drive complete wetting on this substrate, in contrast to Silwet-L77 (Figure 1c), unless a substrate with a higher attraction of hydrophobic headgroups is chosen.

To investigate the influence of the interactions between different chemical groups, we perform simulations where the hydrophobic siloxane beads (red beads) of the straightened Silwet-L77 surfactant are "transmuted" to alkyl groups while keeping the same number of effective beads. This new surfactant molecule resembles a conventional polyalkylether nonionic surfactant (Figure 1j−l), which is manifestly not a superspreader[12] (Figure 1l). Moreover, a significant amount of surfactant remains in the bulk of the droplet, and no evidence of bilayer formation is seen at the CL.

Finally, if one were to arrange the beads of the conventional polyalkylether surfactant into a T-shaped geometry similar to that of Silwet-L77, one again does not observe superspreading behavior. Moreover, a bilayer does not form, despite the T-shaped geometry of the surfactant, which is often considered to be responsible for the formation of bilayers and superspreading. It becomes evident that the surfactant architecture plays a secondary role in superspreading as compared to the surfactant chemistry, which governs the interactions between the surfactant and the substrate and drives bilayer formation, which are concomitant requirements for the superspreading process.

The molecular nature of the model allows for the role of the adsorption/desorption dynamics to be assessed. We define the absolute difference between a specific adsorption and the corresponding desorption, normalized by the spreading time, as a "tendency", F, of the surfactant to move toward different regions of the droplet, i.e., a rate of mass transport. As shown in Figure 2, the "tendency" F associated with the various interfaces, as well as the CL, depends on the surfactant concentration, which is expressed as multiples of the CAC (details in Supporting Information). The inset of Figure 2 illustrates the configurations and main adsorption/desorption mechanisms corresponding to the early, intermediate, and late stages of the spreading process. Clearly, the magnitude of F associated with the transfer from the bulk to the liquid−vapor (LV), solid−liquid (SL), and less noticeable from the latter to the CL exhibits a marked increase beyond concentrations

DOI: 10.1021/la5044798
Langmuir 2015, 31, 2304−2309

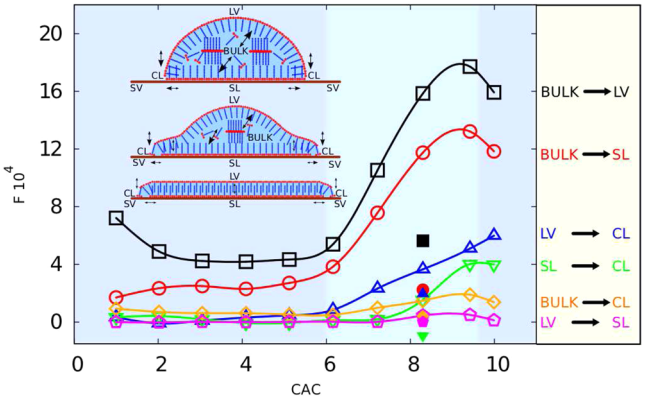

Figure 2. Characterization of the adsorption processes. Nondimensional rate, *F*, characterizing the migration of surfactant molecules between different regions within the droplet. The different interfaces are labeled liquid−vapor (LV), solid−liquid (SL), and contact line (CL). The legend on the right-hand side indicates the color code and the preferential direction of mass transfer. The concentration of surfactant (ordinate) is expressed as a multiple of the critical aggregate concentration (CAC) of the surfactant. Open symbols are given for Silwet-L77 (Figure 1a−c) while solid lines are a guide for the eye. Closed symbols denote the rates for corresponding to the maximum spreading achievable by the conventional surfactant of Figure 1d−f. The superspreading concentration regime (6−9.5CAC) is denoted by a different color. The inset shows from top to bottom three characteristic stages in the superspreading of a droplet, from the initial stage (top), to active advancement and superspreading via the formation of a bilayer at the contact line (middle), to the final stage of complete wetting of the surface (bottom).

approximately equal to 6 × CAC (Figure 2). This increase coincides with an increase in the spreading exponents shown in the inset of Figure 3 that indicates a transition toward rapid spreading, which we interpret as being the onset of superspreading. It is known from experimental observations[14] that

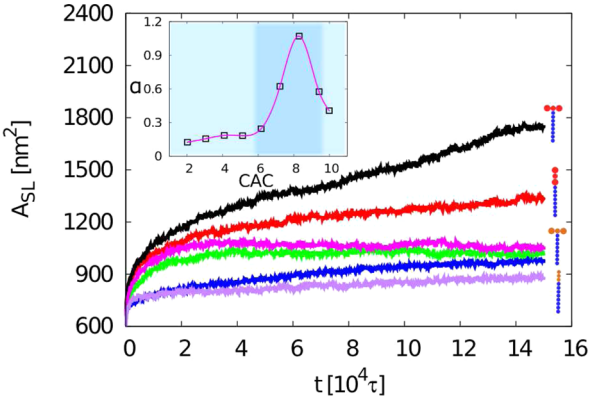

Figure 3. Area of the droplet vs time and spreading rates. Droplet area vs time for the surfactant in Figure 1j−l (purple) and Figure 1 g−i (red) and Silwet-L77 in Figure 1a−c (black). The blue line corresponds to the surfactant in Figure 1d−f. For this surfactant, we exchange the cross interactions of CM effective beads with water beads for the cross interactions of M and D effective beads with water effective beads (green line). We further switch on the cross interactions of M and D effective beads with EO beads, instead of the CM with EO beads (magenta line). The inset shows the characteristic maximum[1] in spreading rates vs concentration for Silwet-L77 (Figure 1a−c), where the superspreading regime is highlighted with a darker color.

Silwet-L77 drives superspreading when present at concentrations above the critical wetting concentration, which corresponds approximately to 7 × CAC, in excellent agreement with our MD results.

A continuum-scale study[10] postulated that the direct adsorption of superspreaders onto the CL plays a fundamental role in superspreading. We observe visual evidence of this mechanism (Supporting Information video); the affinity of Silwet-L77 for adsorption at the CL can be rationalized because the latter is a most-favorable region energetically for surfactants in which their hydrophobic part can avoid contact with water molecules while keeping in contact with the solid substrate and air. The classical description of superspreading surfactants in terms of a hydrophobic head/hydrophilic tail fails to take into account the complexity in the interactions. The perpendicular (T-shaped) placement of the siloxane groups in the surfactant molecule favors their placement and assembly at both SL and liquid−vapor interfaces. This leaves the hydrophilic tails pointing toward the bulk liquid (dominated by the presence of water molecules) or perpendicular to the substrate, favoring a nanolayer of water to form above the substrate. It follows from this that the self-assembly into a bilayer, where water is sandwiched between surfactant layers, is a preferred configuration from both an entropic and an enthalpic point of view, in agreement with experimental results.[33]

As the spreading evolves, increasing the perimeter of the droplet, a larger number of surfactant molecules belong to the CL. In addition to surfactant from the LV surface reaching the CL, there are also surfactant molecules diffusing from the SL interface toward the CL (Figure 2), in agreement with experimental suggestions.[8] Superspreading is crucially dependent on the replenishment of the LV interface as the perimeter of the droplet at the CL increases, hence the argument made in Figure 2 with respect to a requirement that the rates *F* of adsorption both from the bulk to the LV and SL interfaces are crucial, along with a significant increase in the rates *F* of transfer from the interface to the CL. Obviously, an increase in the radius of the drop leads to a rise in the LV and SL interfacial areas by an amount that scales as $(dR)^2$, which is higher than the increase in the droplet perimeter that scales as dR, where R is the radius of the droplet basis. The increase in these interfacial areas leads to a reduction in the respective concentrations; the latter is accentuated further by the direct adsorption at the CL. In order to sustain continuous spreading of the droplet, these interfacial surfactant deficiencies must be replenished rapidly via diffusion from the bulk. This, in turn, is facilitated by the presence of a surfactant "reservoir" in the bulk; therefore, as seen in experiments, a surfactant concentration several times higher than the CAC is necessary to drive complete wetting (Figure 1c).[14] As shown in Figure 2, however, and also in agreement with experimental data,[1] concentrations higher than a certain range reduce the driving force for diffusion toward the interfaces, resulting in slower interfacial replenishment and a decrease in the magnitude of *F* associated with the LV and SL interfaces. Thus, an optimal range of concentration (6−9CAC) exists in which *F* for the CL and the LV and SL interfaces is large. This mechanistic view explains the maximum in the spreading rates vs surfactant concentration curve[1] shown in the inset of Figure 3. Finally, when the droplet attains its ultimate thin film shape (Figure 1c), a dynamic equilibrium among all of the adsorption processes present in the droplet exists: surfactant interchanges

DOI: 10.1021/la5044798
Langmuir 2015, 31, 2304−2309

between the LV surface and the SL interface either through the CL (inset of Figure 2) or directly.

Differences between superspreading and nonsuperspreading surfactants can be identified through an inspection of the adsorption processes. Although the adsorption of surfactant from the LV or SL interfaces to the CL remains significant for the T-shaped alkyl-ether surfactant (Figures 1d−f and 2), the adsorption from the bulk to the interfaces is significantly lower compared to that in the case of Silwet-L77 (Figure 2). This further underlines the importance of rapid interfacial surfactant replenishment and the relative significance of surfactant chemistry over molecular architecture in driving superspreading. A similar comparison between T-shaped (Figure 1a−c) and linear (Figure 1g−i) trisiloxane surfactants shows that adsorption from LV to the CL is multiple times higher in the case of the T-shaped surfactant, while adsorptions from the bulk to the LV and SL interfaces are about 25% higher.

To elucidate yet further the contrasting behavior between the superspreading ability of Silwet-L77 and the conventional behavior of typical nonionic surfactants, we investigate the influence of the chemistry of different surfactant chemical groups. We first consider the linear nonsuperspreading surfactant whose behavior we examined briefly above (Figure 1d−f) and replace the effective alkyl head beads of this surfactant with siloxane beads used within the Silwet-L77 model, observing (Figure 3) a considerably higher spreading rate and area as compared to those of the original linear alkyethoxylated surfactant. The larger size and enhanced dispersion forces of the siloxane headgroup seem to be important for superspreading because they will promote strong adhesion to the substrate and the formation of tight self-assembled surface layers. These interactions, coupled with the antagonism of the headgroups toward water (and the affinity of the tails toward water), enable Silwet-L77 to drag water molecules toward the CL (Figure 2 inset). Subsequently, the LV surface slides on the SL interface, creating the bilayer (Figure 1b) which is crucially absent in the case of a common surfactant (Figure 1j−l).

On the basis of the above systematic study, we have harnessed our understanding of the key "ingredients" of superspreading to design a surfactant molecule that outperforms currently available superspreaders. This molecule has four hydrophobic beads (M) around the hydrophobic bead (D) connected to the hydrophilic tail. We have found that this surfactant increases the spreading rate by 15% compared to the Silwet-L77 surfactant. This molecule appears to offer more efficient shielding of the water molecules from the hydrophobic substrate and a higher probability of adsorption at the CL onto the substrate, while it carries all of the advantages of the Silwet-L77 surfactant.

CONCLUSIONS

Our computer simulations have confirmed and quantified the pivotal elements of the superspreading mechanism and have highlighted the primary differences between superspreading and nonsuperspreading surfactants. The adsorption of surfactants from the LV interface onto the substrate through the CL with the immediate replenishment of the LV and SL interfaces from the bulk are the two indispensable and interlinked mechanisms required for superspreading. It follows that one requires a sufficiently large surfactant concentration, several times the CAC, for effective mass transport. Exceedingly high concentrations, however, reduce bulk diffusion and interfacial surfactant replenishment; thus, superspreading does not occur for this concentration range. The slow replenishment of interfaces with surfactant coming from the bulk and the incapacity of surfactants to replenish the interfaces quickly and self-assemble in a tight structure are the main causes of the nonsuperspreading behavior of conventional nonionic surfactants. These incomplete surface structures are incapable of sliding off of the contact line into an advancing bilayer, which is the other main component of the superspreading mechanism. We anticipate that our results will generate advances in application areas that require control of wetting through the rational design of the mentioned superspreading surfactants using the manipulation of both the chemistry and the molecular architecture.

ASSOCIATED CONTENT

Supporting Information

Methods used in this work and further results related to the validation of the model with experiments. This material is available free of charge via the Internet at http://pubs.acs.org.

AUTHOR INFORMATION

Corresponding Author

*E-mail: o.matar@imperial.ac.uk.

Notes

The authors declare no competing financial interest.

ACKNOWLEDGMENTS

We gratefully acknowledge funding for our work provided by the Engineering and Physical Sciences Research Council (EPSRC), U.K., through grants EP/J010502, EP/I018212, EP/J014958, and EP/L020564. We express our gratitude to N. Kovalchuk and V. Starov from the University of Loughborough for fruitful discussions. We also thank Sadia Rahman for providing the SAFT parameters for the siloxane groups.

REFERENCES

(1) Hill, R. M. Superspreading. *Curr. Opin. Colloid Interface Sci.* **1998**, *3*, 247−254.
(2) Nikolov, A.; Wasan, D. Superspreading mechanisms: An overview. *Eur. Phys. J.: Spec. Top.* **2011**, *197*, 325−341.
(3) Schwarz, E. G.; Reid, W. G. Surface active agents - their behavior and industrial use. *Ind. Eng. Chem.* **1964**, *56*, 26−35.
(4) Venzmer, J. Superspreading - 20 years of physicochemical research. *Curr. Opin. Colloid Interface Sci.* **2011**, *16*, 335−343.
(5) Theodorakis, P. E.; Müller, E. A.; Craster, R. V.; Matar, O. K. Insights into surfactant-assisted superspreading. *Curr. Opin. Colloid Interface Sci.* **2014**, *19*, 283−289.
(6) Ananthapadmanabhan, K. P.; Goddard, E. D.; Chandar, P. A. A study of the solution, interfacial and wetting properties of silicone surfactants. *Colloids Surf.* **1990**, *44*, 281−297.
(7) Ruckenstein, E. Effect of short range interactions on spreading. *J. Colloid Interface Sci.* **1996**, *179*, 136−142.
(8) Ruckenstein, E. Superspreading: A possible mechanism. *Colloids Surf., A* **2012**, *412*, 36−37.
(9) Matar, O. K.; Craster, R. V. Dynamics of surfactant-assisted spreading. *Soft Matter* **2009**, *5*, 3801−3809.
(10) Karapetsas, G.; Craster, R. V.; Matar, O. K. On surfactant-enhanced spreading and superspreading of liquid drops on solid surfaces. *J. Fluid Mech.* **2011**, *670*, 5−37.
(11) Semenov, S.; Trybala, A.; Agogo, H.; Kovalchuk, N.; Ortega, F.; Rubio, R. G.; Starov, V. M.; Velarde, M. G. Evaporation of droplets of surfactant solutions. *Langmuir* **2013**, *29*, 10028−36.
(12) Ivanova, N. A.; Zhantenova, Z. B.; Starov, V. M. Wetting dynamics of polyoxyethylene alkyl ethers and trisiloxanes in respect of

DOI: 10.1021/la5044798
Langmuir 2015, 31, 2304−2309

polyoxyethylene chains and properties of substrates. *Colloids Surf., A* **2012**, *413*, 307−313.
(13) Radulovic, J.; Sefiane, K.; Shanahan, M. E. On the effect of pH on spreading of surfactant solutions on hydrophobic surfaces. *J. Colloid Interface Sci.* **2009**, *332*, 497−504.
(14) Ivanova, N.; Starov, V.; Rubio, R.; Ritacco, H.; Hilal, N.; Johnson, D. Critical wetting concentrations of trisiloxane surfactants. *Colloids Surf., A* **2010**, *354*, 143−148.
(15) Svitova, T.; Hill, R. M.; Smirnova, Y.; Stuermer, A.; Yakubov, G. Wetting and interfacial transitions in dilute solutions of trisiloxane surfactants. *Langmuir* **1998**, *14*, 5023−5031.
(16) Radulovic, J.; Sefiane, K.; Shanahan, M. E. R. Ageing of trisiloxane solutions. *Chem. Eng. Sci.* **2010**, *65*, 5251−5255.
(17) Rosen, M. J.; Wu, Y. Superspreading of trisiloxane surfactant mixtures on hydrophobic surfaces. 1. Interfacial adsorption of aqueous trisiloxane surfactant-N-alkyl-pyrrolidinone mixtures on polyethylene. *Langmuir* **2001**, *17*, 7296−7305.
(18) Rosen, M. J.; Wu, Y. Superspreading of trisiloxane surfactant mixtures on hydrophobic surfaces 2. Interaction and spreading of aqueous trisiloxane surfactant-N-alkyl-pyrrolidinone mixtures in contact with polyethylene. *Langmuir* **2002**, *18*, 2205−2215.
(19) Radulovic, J.; Sefiane, K.; Shanahan, M. E. R. Spreading and Wetting Behaviour of Trisiloxanes. *J. Bionic Eng.* **2009**, *6*, 341−349.
(20) Ivanova, N. A.; Starov, V. M. Wetting of low free energy surfaces by aqueous surfactant solutions. *Curr. Opin. Colloid Interface Sci.* **2011**, *16*, 285−291.
(21) Halverson, J. D.; Maldarelli, C.; Couzis, A.; Koplik, J. Wetting of hydrophobic substrates by nanodroplets of aqueous trisiloxane and alkyl polyethoxylate surfactant solutions. *Chem. Eng. Sci.* **2009**, *64*, 4657−4667.
(22) Shen, Y.; Couzis, A.; Koplik, J.; Maldarelli, C.; Tomassone, M. S. Molecular dynamics study of the influence of surfactant structure on surfactant-facilitated spreading of droplets on solid surfaces. *Langmuir* **2005**, *21*, 12160−12170.
(23) Sergi, D.; Scocchi, G.; Ortona, A. Coarse-graining MARTINI model for molecular-dynamics simulations of the wetting properties of graphitic surfaces with non-ionic, long-chain, and T-shaped surfactants. *J. Chem. Phys.* **2012**, *137*, 094904.
(24) Müller, E. A.; Jackson, G. Force field parameters from the SAFT-γ equation of state for use in coarse-grained molecular simulations. *Annu. Rev. Chem. Biomol. Eng.* **2014**, *5*, 405−427.
(25) Anderson, J. A.; Lorenz, C. D.; Travesset, A. A general purpose molecular dynamics simulations fully implemented on graphics processing units. *J. Comput. Phys.* **2008**, *227*, 5342−5359.
(26) Lobanova, O.; Avendaño, C.; Latte, T.; Müller, E. A.; Jackson, G. SAFT-γ force field for the simulation of molecular fluids. 4. A single-site coarse-grained model of water applicable over a wide temperature range. *Mol. Phys.* **2015**, DOI: 10.1080/00268976.2015.1004804.
(27) Lobanova, O. *Development of Coarse-Grained Force Fields from a Molecular Based Equation of State for Thermodynamic and Structural Properties of Complex Fluids*. Ph.D. Thesis, Imperial College, London, 2014.
(28) Lafitte, T.; Apostolakou, A.; Avendaño, C.; Galindo, A.; Adjiman, C. S.; Müller, E. A.; Jackson, G. Accurate statistical associating fluid theory for chain molecules formed from Mie segments. *J. Chem. Phys.* **2013**, *139*, 154504.
(29) Brini, A.; Algaer, E. A.; Ganguly, P.; Li, C.; Rodrguez-Ropero, F.; van der Vegt, N. F. A. Systematic coarse-graining methods for soft matter simulations a review. *Soft Matter* **2013**, *9*, 2108−2119.
(30) Marrink, S. J.; Risselada, H. J.; Yefimov, S.; Tieleman, D. P.; de Vries, A. H. The MARTINI force field: coarse grained model for biomolecular simulations. *J. Phys. Chem. B* **2007**, *111*, 7812−7824.
(31) Herdes, C.; Santiso, E. E.; James, C.; Eastoe, J.; Müller, E. A. Modelling the interfacial behaviour of dilute light-switching surfactant solutions. *J. Colloid Interface Sci.* **2015**, *445*, 16−23.
(32) Forte, E.; Haslam, A. J.; Jackson, G.; Müller, E. A. Effective coarse-grained solid-fluid potentials and their application to model adsorption of fluids on heterogeneous surfaces. *Phys. Chem. Chem. Phys.* **2014**, *16*, 19165−19180.
(33) Tiberg, F.; Cazabat, C.-M. Self-assembly and spreading of non-ionic trisiloxane surfactants. *Europhys. Lett.* **1994**, *25*, 205−210.

DOI: 10.1021/la5044798
Langmuir 2015, 31, 2304−2309